Sarcoplasmic reticulum Ca^{2+} permeation explored from the lumen side in *mdx* muscle fibers under voltage control

Gaëlle Robin,[1,2] Christine Berthier,[1,2] and Bruno Allard[1,2]

[1]Université Lyon 1, Centre National de la Recherche Scientifique UMR 5534, Centre de Génétique et de Physiologie Moléculaire et Cellulaire, 69622 Villeurbanne Cedex, France
[2]Université de Lyon, 69361 Lyon, Cedex 07, France

Under resting conditions, external Ca^{2+} is known to enter skeletal muscle cells, whereas Ca^{2+} stored in the sarcoplasmic reticulum (SR) leaks into the cytosol. The nature of the pathways involved in the sarcolemmal Ca^{2+} entry and in the SR Ca^{2+} leak is still a matter of debate, but several lines of evidence suggest that these Ca^{2+} fluxes are up-regulated in Duchenne muscular dystrophy. We investigated here SR calcium permeation at resting potential and in response to depolarization in voltage-controlled skeletal muscle fibers from control and *mdx* mice, the mouse model of Duchenne muscular dystrophy. Using the cytosolic Ca^{2+} dye Fura2, we first demonstrated that the rate of Ca^{2+} increase in response to cyclopiazonic acid (CPA)–induced inhibition of SR Ca^{2+}-ATPases at resting potential was significantly higher in *mdx* fibers, which suggests an elevated SR Ca^{2+} leak. However, removal of external Ca^{2+} reduced the rate of CPA-induced Ca^{2+} increase in *mdx* and increased it in control fibers, which indicates an up-regulation of sarcolemmal Ca^{2+} influx in *mdx* fibers. Fibers were then loaded with the low-affinity Ca^{2+} dye Fluo5N-AM to measure intraluminal SR Ca^{2+} changes. Trains of action potentials, chloro-m-cresol, and depolarization pulses evoked transient Fluo5N fluorescence decreases, and recovery of voltage-induced Fluo5N fluorescence changes were inhibited by CPA, demonstrating that Fluo5N actually reports intraluminal SR Ca^{2+} changes. Voltage dependence and magnitude of depolarization-induced SR Ca^{2+} depletion were found to be unchanged in *mdx* fibers, but the rate of the recovery phase that followed depletion was found to be faster, indicating a higher SR Ca^{2+} reuptake activity in *mdx* fibers. Overall, CPA-induced SR Ca^{2+} leak at −80 mV was found to be significantly higher in *mdx* fibers and was potentiated by removal of external Ca^{2+} in control fibers. The elevated passive SR Ca^{2+} leak may contribute to alteration of Ca^{2+} homeostasis in *mdx* muscle.

INTRODUCTION

Duchenne muscular dystrophy is a very severe muscle disease that is characterized by progressive skeletal muscle wasting. Duchenne muscular dystrophy is provoked by mutations in the gene encoding the protein dystrophin, which lead to the total absence of this protein in skeletal muscles. In normal skeletal muscle, dystrophin is located underneath the sarcolemma, and interacts with the F-actin component of the intracellular cytoskeleton at its N-terminal extremity and with a sarcolemmal-embedded glycoprotein complex at its C-terminal extremity, which itself is associated with the extracellular matrix (Blake et al., 2002). Lack of dystrophin is assumed to destabilize this architecture and to promote disruption of the linkage between the subsarcolemmal cytoskeleton and the extracellular matrix, but the functional consequences of the absence of dystrophin that contribute to muscle degeneration still remain elusive. Mainly with the help of the *mdx* mouse model, which also lacks dystrophin, several studies have nevertheless put forward the idea that degeneration of dystrophin-deficient skeletal muscle may result from a chronic intracellular Ca^{2+} overload that initiates massive protein degradation (Mallouk et al., 2000; Gailly, 2002; Ruegg et al., 2002; Allen et al., 2010). Several lines of evidence support the notion that this Ca^{2+} overload is the consequence of a chronic and exacerbated sarcolemmal Ca^{2+} influx. Initially, this Ca^{2+} influx was described to occur through spontaneously active leaky channels or through mechano-gated channels that become overactive in the absence of dystrophin (Fong et al., 1990; Franco and Lansman, 1990; Allard, 2006). More recently, up-regulated store-operated Ca^{2+} entry (SOCE) has been proposed to correspond to the Ca^{2+} influx pathway that contributes to detrimental Ca^{2+} excess in dystrophic muscle fibers (Vandebrouck et al., 2002; Boittin et al., 2006; Edwards et al., 2010). SOCE is thought to be triggered by Ca^{2+} depletion within the SR so that up-regulation of SOCE in dystrophic muscle implies that either SOCE is hyperactive or hypersensitive to SR depletion or that SR depletion is more pronounced in dystrophin-deficient muscle. In support of the

Correspondence to Bruno Allard: bruno.allard@univ-lyon1.fr

Abbreviations used in this paper: CmC, 4-chloro-m-cresol; CPA, cyclopiazonic acid; DHPR, dihydropyridine receptor; SOCE, store-operated Ca^{2+} entry.

The Rockefeller University Press $30.00
J. Gen. Physiol. Vol. 139 No. 3 209–218
www.jgp.org/cgi/doi/10.1085/jgp.201110738

first possibility, Orai1 associated to stromal interacting molecule 1 (STIM1) and the transient receptor potential canonical 1 (TRPC1), two candidate molecules that have been proposed to support SOCE, were found to be overexpressed in *mdx* muscle fibers (Gervásio et al., 2008; Edwards et al., 2010). Possible reduced SR Ca^{2+} content provoked either by an enhanced SR Ca^{2+} leak or by a decreased SR Ca^{2+} filling process has also been investigated in dystrophic muscle, but the results obtained were contradictory. Using chemically skinned muscle fibers, Takagi et al. (1992) first reported an increased SR Ca^{2+} leak in *mdx* muscle with no change in SR Ca^{2+} uptake, whereas Divet and Huchet-Cadiou (2002) described a reduced SR Ca^{2+} uptake and an increased SR Ca^{2+} leak in *mdx* muscle. Using mechanically skinned fibers, Plant and Lynch (2003) reported no difference in SR Ca^{2+} reloading and in the SR Ca^{2+} leak between control and *mdx* muscle fibers. However, because of the loss of intracellular components, skinned fibers do not reproduce the native intracellular environment of the SR so that leakage could be distorted. Intracellular Ca^{2+} sparks at rest, which are thought to reflect a resting SR Ca^{2+} leak, have also been measured in intact and in permeabilized muscle fibers from control and *mdx* mice. Wang et al. (2005) showed that osmotic shock induced irreversible intracellular Ca^{2+} spark activity in intact muscle fibers from *mdx* mice, likely to cause an enhanced SR Ca^{2+} leak, and more recently the frequency of spontaneous Ca^{2+} sparks in permeabilized fibers was found to be significantly higher in *mdx* as compared with control muscle (Bellinger et al., 2009). Nevertheless these experiments were performed in the absence of voltage control. Yet it has been demonstrated that the dihydropyridine receptor (DHPR), whose conformation changes elicited by depolarization promote the opening of the SR Ca^{2+} release channel, regulates the SR passive leak (Eltit et al., 2011). These data suggest that muscle membrane potential may control not only SR active Ca^{2+} release but also SR passive Ca^{2+} leak, further emphasizing the need to control membrane potential to carefully investigate the SR Ca^{2+} permeation process.

In this paper, we investigate SR Ca^{2+} permeation at resting potential in intact voltage-controlled skeletal muscle fibers from control and *mdx* mice. Using cytosolic and intraluminal SR Ca^{2+} dyes, we demonstrate that the passive SR Ca^{2+} leak is significantly higher in *mdx* fibers and is associated with an elevated SR Ca^{2+} reuptake activity and a likely up-regulation of SOCE. Our study also shows that SR Ca^{2+} depletion induced by depolarizing pulses of controlled amplitude is not altered in dystrophin-deficient fibers.

MATERIALS AND METHODS

Preparation of muscle fibers

All experiments were performed in accordance with the guidelines of the French Ministry of Agriculture (87/848) and of the European Community (86/609/EEC). Interosseal and fdb (flexor digitorum brevis) muscles were removed from 1–2-mo-old male C57BL6 or OF1 (as indicated in the figure legends) and *mdx-5cv* mice. Single skeletal muscle fibers were isolated by a 50-min enzymatic treatment at 37°C using a Tyrode solution containing 2 mg/ml collagenase type I (Sigma-Aldrich).

Electrophysiology

The major part of a single fiber was electrically insulated with silicone grease, and a micropipette was inserted into the fiber through the silicone layer to current clamp or voltage clamp the portion of the fiber free of grease (50–100 µm in length) using a patch-clamp amplifier (RK-400; Bio-Logic) in a whole-cell configuration (Pouvreau et al., 2007). Command voltage or current pulse generation and data acquisition were done using the pClamp10 software (Axon Instruments) driving an A/D converter (Digidata 1400A; Axon Instruments). Analogue compensation was systematically used to decrease the effective series resistance. Currents or membrane potentials were filtered at 3 kHz and acquired at a sampling frequency of 10 kHz. The tip of the micropipette was then crushed into the dish bottom to allow intracellular dialysis of the fiber with the intra-pipette solution (see Solutions; Berbey and Allard, 2009).

Measurements of cytosolic Ca^{2+} using Fura-2

Cells were dialyzed through the micropipette during 20 min using an intracellular solution containing 100 µM Fura-2. Fura-2 was excited at 340 and 380 nm, and fluorescence was measured between 520 and 560 nm on images from a region of 20 µm diameter on the silicone-free extremity of the cell. Images were captured with a charge-coupled device camera (Roper Scientific) driven by the Metavue software and using a 40× oil immersion objective. After background subtraction, the ratio F340/F380 was calculated to estimate $[Ca^{2+}]$. Images were captured at a frequency of 0.5 Hz to limit photobleaching.

Confocal microscopy

Subcellular distribution of Fluo-5N was observed with a confocal microscope (LSM 5; Carl Zeiss) using a 63× oil immersion objective lens.

Measurements of Ca^{2+} in SR lumen using Fluo-5N

Fibers were incubated in a Tyrode solution containing 10 µM Fluo-5N in the acetoxymethyl ester form at room temperature for 2 h to allow entry of the dye into the SR, and subsequent deesterification. Cells were then dialyzed for 20 min through the micropipette used for voltage clamping with an internal solution containing 50 mM EGTA (see Solutions) to prevent contraction during imaging and avoid possible contribution of cytosolic Ca^{2+} changes to SR Ca^{2+} signals. Fluo-5N was excited at 488 nm, and the emitted fluorescence was measured at 520 nm after background subtraction. Changes in SR Ca^{2+} content were expressed as F/F_0, where F_0 is the measured fluorescence at the steady state at the beginning of the experiment. The frequency of images capture ranged between 0.2 and 25 Hz depending on the recording duration. For each experiment, this frequency is indicated in the figure legends.

Solutions

For experiments using Fura-2 and experiments using Fluo-5N under current clamp conditions, the Tyrode external saline contained 140 mM NaCl, 5 mM KCl, 2.5 mM $CaCl_2$ (or 0, compensated by 2.5 mM $MgCl_2$), 2 mM $MgCl_2$, and 10 mM Hepes adjusted to pH 7.2 with NaOH. For experiments using Fluo-5N under voltage clamp conditions, the external solution contained 140 mM TEA-methanesulfonate, 2.5 mM $CaCl_2$, 2 mM $MgCl_2$, and 10 mM Hepes adjusted to pH 7.2 with TEA-OH. For experiments using Fura-2, the intrapipette solution contained 120 mM

potassium glutamate, 5 mM Na_2-ATP, 5 mM Na_2-phosphocreatine, 5.5 mM $MgCl_2$, 5 mM glucose, and 5 mM Hepes adjusted to pH 7.2 with KOH. For experiments using Fluo-5N, the intrapipette solution contained 50 mM EGTA-KOH, 50 mM potassium glutamate, 5 mM Na_2-ATP, 5 mM Na_2-phosphocreatine, 5.5 mM $MgCl_2$, 5 mM glucose, and 5 mM Hepes adjusted to pH 7.2 with KOH. Stock solution of Fura-2 was dissolved in distilled water at 10 mM. Stock solutions of Fluo-5N AM, 4-chloro-m-cresol (CmC), and cyclopiazonic acid (CPA) were dissolved in dimethylsulfoxide at 1, 1,000, and 50 mM, respectively. Cells were exposed to different solutions by placing them in the mouth of a perfusion tube from which flowed by gravity the rapidly exchanged solutions. Experiments were performed at room temperature.

Statistics

Fits were performed with Microcal Origin software (GE Healthcare). Data are given as means ± SEM and compared using different tests indicated in the figure legends or in the text. Differences were considered significant when $P < 0.05$. In the figures, *, $P < 0.05$; **, $P < 0.005$; ***, $P < 0.0005$.

Online supplemental material

Fig. S1 depicts the intracellular distribution of Fluo-5N in a control fiber using confocal imaging and the corresponding average fluorescence intensity profile from a small region of this fiber. Online supplemental material is available at http://www.jgp.org/cgi/content/full/jgp.201110738/DC1.

RESULTS

Changes in cytosolic Ca^{2+} induced by SR Ca^{2+}-ATPase inhibition in control and *mdx* fibers

In a previous paper, we showed that pharmacological inhibition of the SR Ca^{2+}-ATPases by CPA induced a progressive increase in cytosolic Ca^{2+} at resting potential that mainly results from the passive Ca^{2+} leak from the SR (Berbey et al., 2009). We used this pharmacological tool here to determine if the magnitude of the SR Ca^{2+} leak was different in control and in *mdx* muscle fibers. Fig. 1 A shows that CPA poisoning led to an increase in intracellular Ca^{2+} monitored by Fura-2 at a higher rate in an *mdx* fiber as compared with a control one at a holding potential of −80 mV. Fitting a linear regression to the fluorescence records 1 min after CPA addition in every cell tested indicated that the mean rate of fluorescence increase was significantly higher in *mdx* (0.51 ± 0.07 ratio [F340/F380]/min) as compared with control fibers (0.11 ± 0.01 ratio [F340/F380]/min; Fig. 1 B), which suggests that SR Ca^{2+} leak is higher in dystrophin-deficient fibers. However, it cannot be excluded that an influx of external Ca^{2+} contributed to the measured Ca^{2+} changes, as the Ca^{2+} leak from the SR, no longer compensated for by Ca^{2+} uptake, may be responsible for a substantial depletion of Ca^{2+} in the SR that in turn may activate SOCE. Thus, in order to exclude the contribution of SOCE to CPA-induced cytosolic Ca^{2+} increase and focus on the SR Ca^{2+} leak, fibers were bathed in a Ca^{2+}-free external solution before the addition of CPA. Unexpectedly, under these conditions of continuous exposure of fibers to the Ca^{2+}-free medium, the rate of CPA-induced Ca^{2+} increase was significantly augmented in control fibers, whereas it was significantly decreased in *mdx* fibers (Fig. 1 B). There was also no significant difference in the rate of CPA-induced Ca^{2+} increase between control and *mdx* fibers in the Ca^{2+}-free medium. Collectively, these data suggest that removal of external Ca^{2+} has important effects on intracellular Ca^{2+} handling that are not simply limited to suppression of SOCE, and provokes an increase in the SR Ca^{2+} leak (see results in Fig. 6 A). To further investigate the SR Ca^{2+} leak in control and in *mdx* fibers, and to circumvent the use of Ca^{2+}-free solution for preventing the possible involvement of SOCE, we next investigated SR Ca^{2+} permeation by measuring the changes in intraluminal Ca^{2+} using a low-affinity Ca^{2+} dye loaded in the SR.

Monitoring of Ca^{2+} changes in the SR lumen of control fibers

After loading of the dye, confocal images revealed a striated pattern of Fluo-5N fluorescence (Fig. S1). A fluorescence profile of a selected region revealed the presence of doublets consistent with accumulation of the de-esterified form of the dye mainly at the level of the junctional SR (Fig. S1). The presence of the dye in

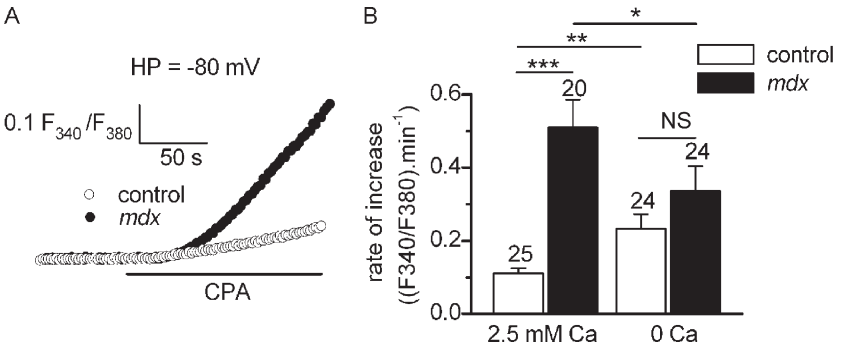

Figure 1. Changes in cytosolic Ca^{2+} induced by SR Ca^{2+}-ATPase inhibition in control and in *mdx* fibers. (A) Changes in intracellular Ca^{2+} monitored by Fura-2 and induced by 50 µM CPA in a control (C57BL6 mouse) and in an *mdx* fiber at a holding potential of −80 mV (the fluorescence baselines before addition of CPA were superimposed to make easier the comparison of the fluorescence changes induced by CPA in the two fiber types). (B) Mean rates of CPA-induced Ca^{2+} changes in control (C57BL6 mice) and in *mdx* fibers in the presence of 2.5 mM Ca^{2+} or in the absence of Ca^{2+} in the external solution. The numbers above each bar indicate the number of cells tested. Mean values in control and in *mdx* fibers and mean values in the presence of Ca^{2+} and in its absence have been compared using a Student's unpaired *t* test. *, $P < 0.05$; **, $P < 0.005$; ***, $P < 0.0005$. Error bars indicate mean ± SEM.

the SR lumen was confirmed by measuring the changes in Fluo-5N fluorescence induced by various stimuli of SR Ca^{2+} release in the presence of a high intracellular concentration of EGTA. Fig. 2 A shows that a train of action potentials delivered at 50 Hz during 1 s under the current clamp condition in the presence of Tyrode evoked a marked decrease in Fluo5N fluorescence. Fluorescence had recovered 2 min later, and exposure of the same fiber to 1 mM of the ryanodine receptor agonist CmC at −80 mV gave rise to a decrease in Fluo5N fluorescence of a similar amplitude, which was partially reversible upon washout of the drug (Fig. 2 B).

The Fluo5N signals were explored in more detail under voltage clamp conditions in response to depolarizing pulses of increasing amplitudes in control fibers from OF1 mice. Fig. 3 A shows that depolarizing pulses >−40 mV evoked a drop in Fluo-5N fluorescence, whose magnitude and kinetics increased with the amplitude of the depolarization. For pulses >−20 mV, the decrease in fluorescence was associated with the activation of inward membrane currents that shared all the characteristics of voltage-activated L-type Ca^{2+} currents, routinely recorded in this preparation under similar experimental conditions. The best fit to the mean decrease in Fluo-5N fluorescence as a function of voltage using a Boltzmann equation indicated a $V_{1/2}$ of −23mV, a steepness factor of 3 mV, and a maximal decrease of fluorescence of 40% (Fig. 3 B). The magnitude of the decrease in Fluo5N fluorescence induced by trains of action potentials (52 ± 8%, n = 5), CmC (45 ± 6%, n = 5), and a single voltage pulse to +20 mV (42 ± 4%, n = 12) were found to not be significantly different (Student's unpaired t test).

As already illustrated in Fig. 2, Fig. 3 A shows that, despite the presence of a high intracellular concentration of EGTA, Fluo-5N fluorescence recovery occurred during the 2-min intervals that separated voltage pulses. This recovery phase that followed voltage-activated Fluo-5N fluorescence decrease could be totally inhibited by the presence of the SR Ca^{2+}-ATPase inhibitor CPA. At a holding potential of −80 mV, exposing the fiber to CPA induced a progressive decrease in Fluo-5N fluorescence that likely revealed an SR passive Ca^{2+} leak (see also Fig. 6), no longer balanced by the activity of Ca^{2+}-ATPases (Fig. 4 A). A depolarizing pulse to 0 mV evoked an abrupt decrease in Fluo-5N fluorescence that was maintained during the 50-s duration pulse but also upon repolarization of the fiber. Washout of CPA led to a progressive return of Fluo-5N fluorescence toward its initial level. Collectively, these results indicate that the changes in Fluo-5N fluorescence elicited by depolarizing pulses mainly report decreases in luminal [Ca^{2+}], which results from voltage-activated SR Ca^{2+} release and subsequent depletion. To further examine the recovery phase of Fluo-5N fluorescence after voltage-activated Ca^{2+} release, depolarizing pulses of increasing duration were applied on the same fiber. As illustrated in Fig. 4 B, a first pulse of 1-s duration to +30 mV induced a rapid decrease of Fluo-5N fluorescence, which remained stable during depolarization and which was then followed upon repolarization at −80 mV by a fast recovery phase (τ = 1.4 s in this cell). 2 min later, Fluo-5N fluorescence had returned to the initial level, and a second, longer pulse of 5-s duration gave rise to a comparable initial drop in fluorescence, but this time followed, after a 1-s stabilization, by a recovery phase approximately five times slower during depolarization (τ = 4.8 s) than during repolarization. Upon repolarization to −80 mV, Fluo-5N fluorescence rapidly recovered with a kinetic measurement similar to the one measured after the first 1 s-pulse (τ = 1 s). Finally a third pulse maintained during 20 s gave rise to a change in Fluo-5N fluorescence of similar amplitude and kinetics compared with the one measured during the 5-s pulse, except that repolarization after a 20-s depolarization did not induce any change in the recovery phase kinetic. Similar results were obtained in two other cells. These data likely indicate that depolarization leads to SR depletion that is maintained as long as SR Ca^{2+} release channels remain open, and slowly recovers because of the progressive

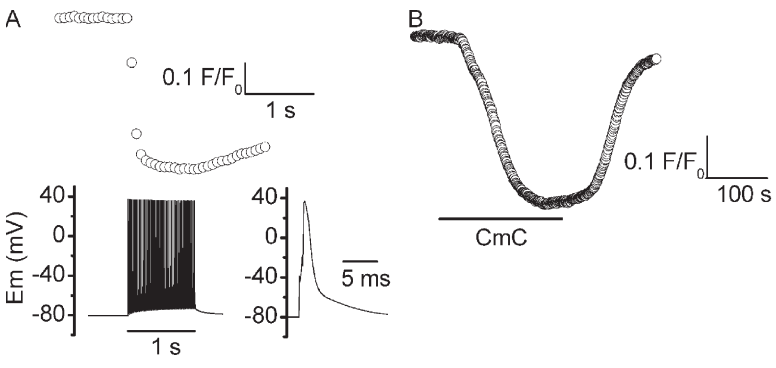

Figure 2. Changes in Fluo-5N fluorescence induced by a train of action potentials, CmC, and depolarizing pulses. (A) Simultaneous recordings of a train of action potentials (bottom left trace) induced by a burst of supraliminal current pulses, 0.5 ms in duration at a frequency of 50 Hz during 1 s in current clamp conditions, and of the associated changes in Fluo-5N fluorescence (top trace) in the presence of an external Tyrode solution in a control fiber (C57BL6 mouse). The first action potential of the train is shown on an expanded time scale next to the train. (B) Change in Fluo-5N fluorescence induced by exposure of the same fiber as in A 2 min later to 1 mM CmC at a holding potential of −80 mV in current clamp conditions. Fluorescence images were captured at a frequency of 15 Hz in A and 1 Hz in B.

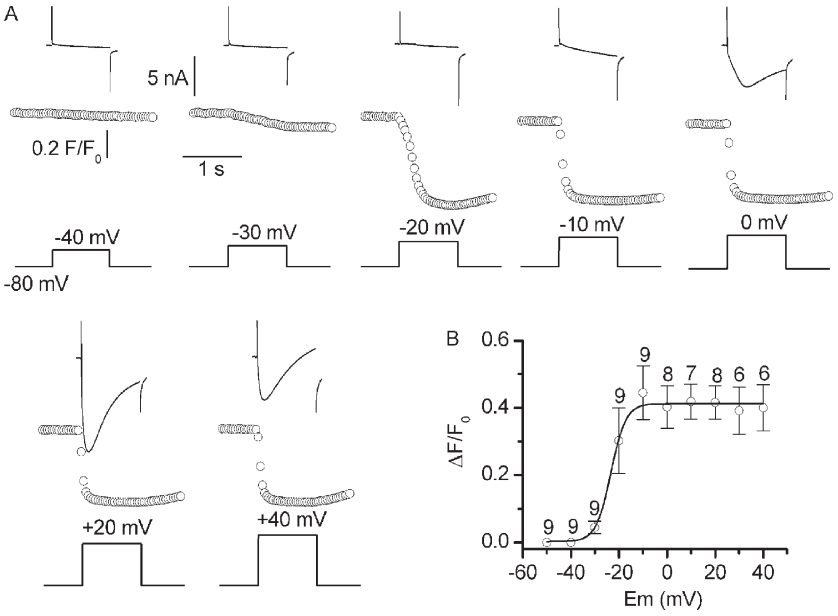

Figure 3. Changes in Fluo-5N fluorescence induced by depolarizing pulses of increasing amplitude. (A) Simultaneous recordings of membrane currents (top trace) and changes in Fluo-5N fluorescence (middle traces) in the same control fiber (OF1 mouse) in response to depolarizing pulses of 1 s duration and increasing amplitudes delivered every 2 min (bottom traces). Images recorded for fluorescence measurements were captured at a frequency of 25 Hz. (B) Relationship between the mean changes in Fluo-5N fluorescence and membrane potential. The change in Fluo-5N fluorescence induced by depolarization corresponds to the measured difference between the minimal value of fluorescence recorded during the voltage pulse and the baseline value before the pulse. The numbers above each data point indicate the number of cells tested. Error bars indicate mean ± SEM.

closure of Ca^{2+} release channels induced by inactivation of excitation–contraction coupling together with SR Ca^{2+} refilling. Upon repolarization or after total inactivation of the Ca^{2+} release channels, the fast recovery phase mainly resulted from the Ca^{2+} reloading process.

Comparison of voltage-induced Ca^{2+} changes in the SR lumen of control and mdx fibers

A set of experiments next aimed at comparing the magnitude, the voltage dependence, and the kinetics of the recovery phase of Ca^{2+} depletion in the SR lumen induced by depolarizing pulses in control (C57BL6 mice) and in *mdx* fibers. Fig. 5 (A and B) shows that the mean maximal amplitude of the voltage-induced Fluo-5N fluorescence decrease (0.29 ± 0.03 $\Delta F/F_0$ in control versus 0.31 ± 0.03 $\Delta F/F_0$ in *mdx* fibers), the $V_{1/2}$ (−22 ± 2.5 mV in control vs. −24 ± 2 mV in *mdx* fibers), and the steepness factor (2.1 ± 0.1 mV in control vs. 2.3 ± 0.4 mV in *mdx* fibers) of the voltage dependence of the depolarization-induced Fluo-5N fluorescence decrease were not significantly different in control and in *mdx* fibers. However, as clearly illustrated in the mean Ca^{2+} signals elicited by voltage pulses in Fig. 5 A, the recovery phase of fluorescence that followed voltage pulses was faster in *mdx* fibers than in control fibers. Because some cells displayed a very slow recovery phase that precluded any satisfactory fitting of the recovery time course with an exponential function, we chose to measure the fraction of fluorescence that had recovered 1 s after the end of the pulse in every cell depolarized between +10 and +40 mV. On average, the fraction of fluorescence recovery was quite significantly higher in *mdx* (26 ± 3%, n = 48) as compared with control fibers (10 ± 2%, n = 44), which suggests that SR Ca^{2+} reuptake subsequent to voltage-induced SR depletion is more efficient in dystrophin-deficient fibers.

Resting SR Ca^{2+} leak in control and in *mdx* fibers

Measurements of cytosolic Ca^{2+} changes in response to CPA poisoning in Fig. 1 indicated that the rate of CPA-induced Ca^{2+} increase was augmented in control

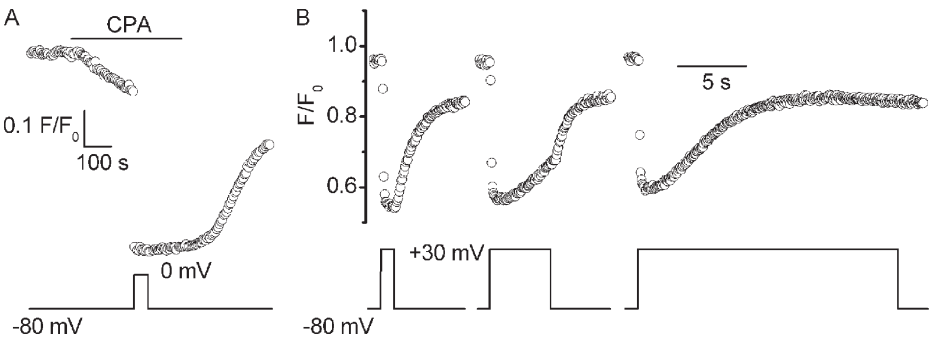

Figure 4. Voltage-induced changes in Fluo-5N fluorescence in response to a single or to successive depolarizing pulses in the presence or absence of CPA. (A) On this representative recording, a muscle fiber was submitted to a 50-s depolarizing pulse to 0 mV in the presence of 50 µM CPA. (B) Three consecutive pulses to +30 mV of 1, 5, and 20 s in duration and separated by 2-min intervals were applied on the same fiber. Fluo-5N fluorescence images were collected at a frequency of 0.2 Hz in A and 15 Hz in B in two control fibers (OF1 mice).

fibers in the absence of external Ca^{2+}, which suggests an increased SR Ca^{2+} leak provoked by the absence of external Ca^{2+}. To test if a potentiating effect of a Ca^{2+}-free external solution could be revealed on the SR Ca^{2+} leak, control fibers were loaded with Fluo-5N, voltage-clamped at −80 mV, and exposed to CPA in the presence and in the absence of external Ca^{2+}. Fig. 6 A shows that in the presence of external Ca^{2+}, CPA induced a progressive decrease in Fluo-5N fluorescence as already presented in Fig. 4 A, the rate of which increased upon removal of external Ca^{2+}. Fitting a linear regression to the fluorescence decline in every cell tested indicated that the mean rate of CPA-induced fluorescence decrease was significantly higher in the absence of external Ca^{2+} (0.056 ± 0.0117 $[F/F_0]$min) than in its presence (0.034 ± 0.0057 $[F/F_0]$/min), which indicates a potentiation of the SR Ca^{2+} leak upon removal of external Ca^{2+} (Fig. 6 B). The rate of CPA-induced Fluo-5N fluorescence decrease was then compared in control and in *mdx* fibers in the presence of external Ca^{2+} (Fig. 6 C). As illustrated in Fig. 6 D, the rate of CPA-induced Fluo-5N fluorescence decrease was found to be significantly doubled in *mdx* as compared with control fibers, which suggests that the passive SR Ca^{2+} leak is higher in dystrophin-deficient fibers.

DISCUSSION

In this paper, we investigated the SR Ca^{2+} leak at resting membrane potential in dystrophin-deficient fibers. Up to now, the SR leak had been explored in isolated SR vesicles, skinned fibers, or intact fibers, though in the absence of voltage control. The use of intact fibers under acute voltage control in the present study allowed us to avoid possible distortion provoked by the loss of intracellular components in isolated SR vesicles or skinned fibers and by uncontrolled voltage-induced SR Ca^{2+} fluxes. Voltage control also offers the advantage of being able to monitor the background membrane current, which, when stabilized to a low level, represents a reliable index of fiber integrity. At a resting state, the Ca^{2+} leak is constantly balanced by the influx of Ca^{2+} into the SR created by the pumps so that inhibition of the SR Ca^{2+}-ATPases reveals, at least in part, the leaky

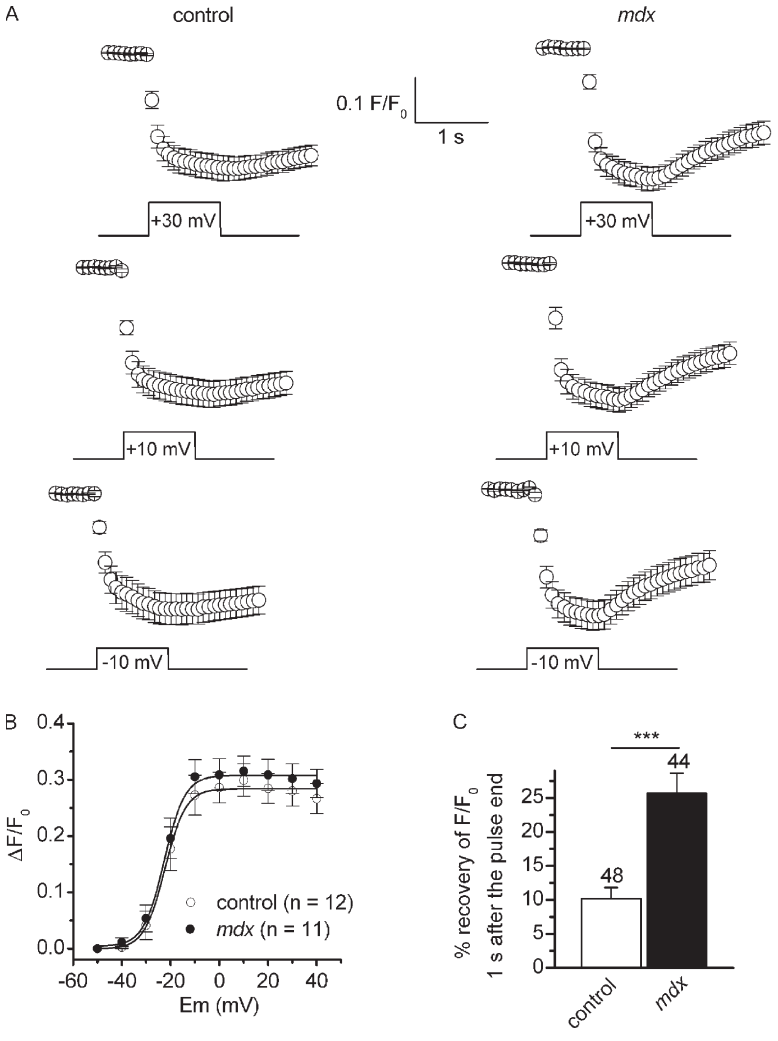

Figure 5. Changes in Fluo-5N fluorescence induced by depolarization in control and in *mdx* fibers. (A) Means and SEM of Fluo-5N fluorescence changes in response to depolarizing pulses to −10, +10, and +30 mV from a holding potential of −80 mV in 12 control (C57BL6 mice; left) and 11 *mdx* (right) fibers. Images were collected at a frequency of 12.5 Hz. (B) Relationship between the mean changes in Fluo-5N fluorescence and membrane potential in control and *mdx* fibers. The changes in Fluo-5N fluorescence were measured as explained in the legend of Fig. 4. (C) Mean percentages of fluorescence recovery 1 s after the end of the depolarizing pulses at +10, +20, +30, and +40 mV in the 12 control and 11 *mdx* fibers. Mean values have been compared using a Student's unpaired *t* test. Error bars indicate mean ± SEM.

efflux of Ca^{2+} from the SR. Our first set of measurements of Ca^{2+} changes in the cytosol indicated that inhibition of the SR pumps by CPA led to an increase in cytosolic [Ca^{2+}] at a very significant higher rate in *mdx* fibers in the presence of physiological external [Ca^{2+}]. However, under these experimental conditions, the SR Ca^{2+} leak induced by CPA may progressively lead to SR Ca^{2+} depletion, which in turn may provoke SOCE activation. The cytosolic Ca^{2+} increase induced by CPA may then result both from Ca^{2+} efflux from the SR and from Ca^{2+} influx through SOCE. However, when cells were bathed in a Ca^{2+}-free external solution to prevent any SOCE contribution to the cytosolic Ca^{2+} changes induced by CPA, the rate of CPA-induced Ca^{2+} increase was augmented in control fibers and decreased in *mdx* fibers. This result suggested that SR Ca^{2+} leak is potentiated in the absence of external Ca^{2+} in control fibers, giving rise to a rate of increase in cytosolic Ca^{2+} that is higher than the one measured in the presence of external Ca^{2+}; i.e., under experimental conditions that allow SOCE to occur. In *mdx* fibers, the observed decrease of the rate of CPA-induced Ca^{2+} increase in the absence of extracellular Ca^{2+}, which did not became significantly different from the rate measured in control fibers in Ca^{2+}-free solution, gives evidence that the higher rate of CPA-induced Ca^{2+} increase in *mdx* fibers in the presence of physiological Ca^{2+} is principally caused by an elevated sarcolemmal influx, likely via SOCE. This interpretation is consistent with the recent data obtained by Edwards et al. (2010) in skinned muscle fibers, which provides evidence for an up-regulation of SOCE in *mdx* muscle. Nevertheless, this series of cytosolic Ca^{2+} measurements on its own did not allow for a straightforward conclusion about the respective contribution of the SR leak and sarcolemmal Ca^{2+} influx in the elevated rate of Ca^{2+} increase in response to CPA poisoning in *mdx* muscle fibers.

To circumvent limitations associated with the use of Ca^{2+}-free external solution, we used a low-affinity Ca^{2+} indicator, Fluo5N, which is able to report Ca^{2+} changes in the SR lumen. Kabbara and Allen (2001) were the first to use Fluo5N to measure SR calcium in muscle fibers of the cane toad, and more recently, Ziman et al. (2010) successfully used this Ca^{2+} dye in mouse skeletal muscle fibers. We obtained here similar confocal images of subcellular distribution of Fluo5N fluorescence as Ziman et al. (2010), which indicates the presence of the indicator mainly in the junctional SR. As mentioned by these authors, after loading, the dye may also have accumulated in the cytosol and in other organelles such as mitochondria. However, the very high internal concentration of EGTA that we used should considerably minimize the possible contamination of the recorded Fluo5N fluorescence by signals originating from non-SR compartments. Overall, we showed that stimuli eliciting SR Ca^{2+} release, such as trains of action potentials, addition of a potent agonist of ryanodine receptors, and depolarization pulses all evoked a transient decrease in Fluo5N fluorescence, demonstrating that Fluo5N mainly reports Ca^{2+} changes in the SR lumen. Although the sampling rate of our fluorescence imaging (25 Hz for the highest) did not allow us to acutely

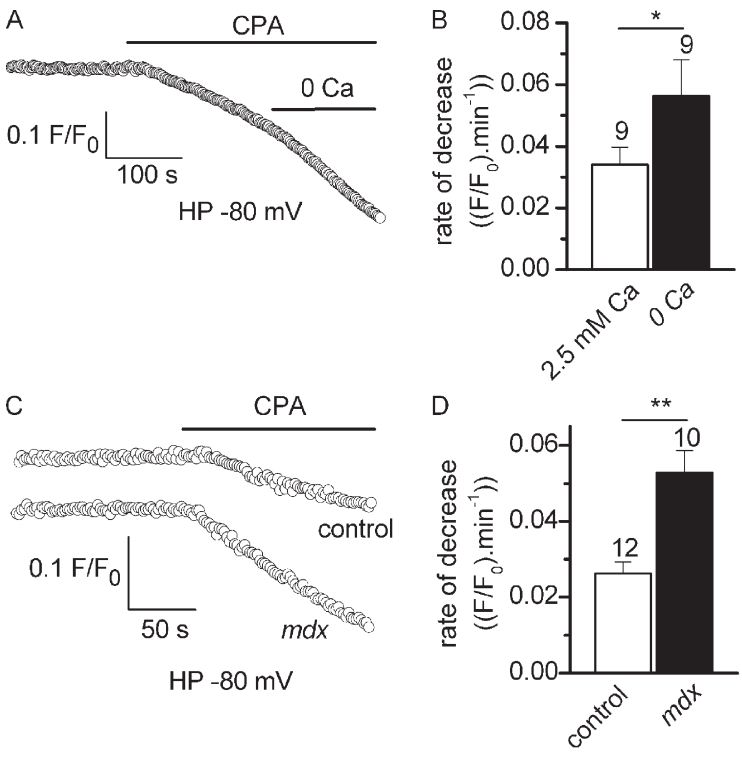

Figure 6. Decrease in Fluo-5N fluorescence induced by CPA in control and in *mdx* fibers. (A) Effect of removal of external Ca^{2+} on the changes in Fluo-5N fluorescence induced by addition of 50 µM CPA in a control (C57BL6 mouse) fiber. (B) Mean rates of CPA-induced fluorescence decrease in the absence and in the presence of 2.5 mM external Ca^{2+}. Mean values have been compared using a Student's paired *t* test. (C) Changes in Fluo-5N fluorescence in response to the addition of 50 µM CPA in a control (C57BL6 mouse) and in an *mdx* fiber. (D) Mean rates of fluorescence decrease in control and in *mdx* fibers. Mean values have been compared using a Student's unpaired *t* test. Images were collected at a frequency of 0.5 Hz in A and C. ***, $P < 0.0005$. Error bars indicate mean ± SEM.

analyze the kinetics of the Fluo5N signal, the profile of our Fluo5N responses induced by 1-s depolarizations were very comparable to the profile of responses of the Ca^{2+} sensor cameleon D4cpv targeted to the SR, recently described by Sztretye et al. (2011), exhibiting a rapid phase of decrease upon depolarization followed by a plateau phase and then a slow recovery phase upon repolarization. The fact that our response profiles matched the ones obtained with cameleon proteins that specifically express in the SR further demonstrates that our Fluo5N signals originate from the SR lumen.

Despite the presence of a high concentration of Ca^{2+} buffer in the cytosol, we also observed that, after depolarization-induced depletion, the SR Ca^{2+} level returned to close to the initial value during the 2-min intervals that separated pulses, and this recovery phase was inhibited by the SR Ca^{2+} pump blocker CPA. Although this recovery phase takes place on a nonphysiological time scale because of the high concentration of EGTA, these data indicate that SR Ca^{2+}-ATPases have the capacity to actively reuptake Ca^{2+} into the SR by overcoming the Ca^{2+}-chelating action of the buffer.

Acute control of the fiber membrane potential allowed us to investigate the voltage dependence of the depolarization-induced SR Ca^{2+} changes. We obtained voltage values of half activation ranging −23 to −22 mV and a steepness factor ranging 2 to 3 mV in the series of experiments performed in fibers from three different mouse lineages. These values are very close to the corresponding values obtained for the voltage dependence of Ca^{2+} release measured with a cytosolic Ca^{2+} indicator and the same silicone clamp technique (Pouvreau et al., 2006). Using the cameleon D1ER to monitor SR Ca^{2+} changes, Jiménez-Moreno et al. (2010) obtained more depolarized values of half activation (∼−15 mV) and less steep voltage dependence (close to 6 mV). However, they also obtained comparable fit parameters for the voltage dependence of Ca^{2+} release measured with a cytosolic Ca^{2+} dye. The use of a different voltage clamp technique in this study, the whole-cell configuration of the patch clamp technique on whole fdb adult muscle fibers, could explain the different values reported for SR Ca^{2+} changes as compared with ours.

Our measurements of voltage-induced Fluo5N decrease performed on *mdx* and C57BL6 control fibers indicated that neither the magnitude of the Ca^{2+} depletion nor its voltage dependence were significantly changed in dystrophin-deficient fibers. This result is in concordance with several studies that reported no significant difference in the amplitude (Turner et al., 1988; Tutdibi et al., 1999) and in the voltage dependence (Collet et al., 1999) of cytosolic Ca^{2+} transients recorded from normal and *mdx* muscles but contrasts with the observations of DiFranco et al. (2008) and Hollingworth et al. (2008), who found a significant reduction of the amplitude of the action potential–evoked Ca^{2+} transients in *mdx* mice. However, the low sampling rate of our SR Ca^{2+} measurements did not allow us to explore the Ca^{2+} signal during the first 50 ms, so we cannot exclude the possibility that a transient phase of depletion that may precede the plateau phase could be altered in *mdx* muscle.

Upon repolarization to −80 mV, we observed a quite significantly faster rate of Fluo5N recovery in *mdx* fibers, which suggests a higher reuptake efficiency of SR Ca^{2+}-ATPases. In the literature, either no change or a reduced velocity of Ca^{2+} reuptake has been described in *mdx* muscle (Turner et al., 1988; Takagi et al., 1992; Kargacin and Kargacin, 1996; Collet et al., 1999; Divet and Huchet-Cadiou, 2002; Plant and Lynch, 2003; Woods et al., 2004). Different experimental conditions might explain the different results obtained. To our knowledge, our study is indeed the first to explore the SR Ca^{2+} reuptake process from the SR lumen side under voltage control in intact fibers. These conditions offer the advantage of preserving the native cellular environment of the SR and avoiding the possible involvement of cytosolic Ca^{2+} binding sites that may compete with cytosolic Ca^{2+} dyes in a different manner in control and *mdx* muscles. The higher reloading efficiency of SR Ca^{2+}-ATPases in dystrophin-deficient fibers may be seen as a compensatory mechanism in response to chronic Ca^{2+} overload and an elevated SR Ca^{2+} leak, as further suggested by our results.

Measurement of Fluo5N fluorescence in the presence of CPA led us to directly monitor the Ca^{2+} leak from the SR lumen at resting membrane potential. We first confirmed that the SR Ca^{2+} leak revealed by CPA poisoning of SR Ca^{2+}-ATPases is significantly increased in the absence of external Ca^{2+}, as suggested by experiments performed using Fura-2. The mechanisms involved in the up-regulation of the SR Ca^{2+} leak in control fibers after external Ca^{2+} removal are not clear. Eltit et al. (2011) proposed that the DHPR regulates the SR passive leak at a resting state. It thus can be postulated that removal of external Ca^{2+} may induce changes in the configuration of the DHPR that could weaken the repressive action exerted by its presence on the leak state of the ryanodine receptor, resulting in an elevated leak. Overall, we demonstrated that CPA-induced SR Ca^{2+} leak occurred at a significant faster rate in *mdx* fibers together with an elevated sarcolemmal influx. This result is in agreement with results obtained in skinned fibers (Takagi et al., 1992; Divet and Huchet-Cadiou, 2002) but also in intact and permeabilized fibers from *mdx* muscles in which a higher frequency of osmotic shock-induced and spontaneous Ca^{2+} sparks was, respectively, reported (Wang et al., 2005; Bellinger et al., 2009). The SR Ca^{2+} leak has been postulated to occur through ryanodine receptors in the absence of releasing signals, but other pathways could be potentially involved (Camello et al., 2002; Guerrero-Hernandez et al., 2010). Among these pathways, the TRPC1 channel is a potential candidate

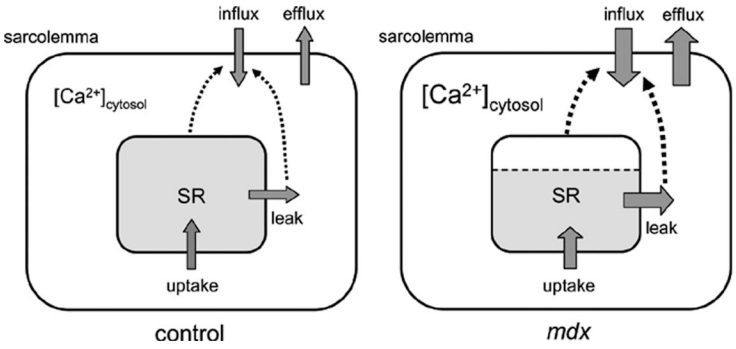

Figure 7. Model showing the Ca^{2+} fluxes in control and *mdx* fibers and the possible consequences of the changing of these fluxes on Ca^{2+} homeostasis in *mdx* fibers. Gray arrows correspond to Ca^{2+} fluxes. Partial filling with gray color of the SR compartment in *mdx* fibers indicates possible reduced SR Ca^{2+} content. Broken black arrows indicate that SR depletion and/or SR leak influence sarcolemmal Ca^{2+} influx and provoke in *mdx* fibers a higher sarcolemmal Ca^{2+} influx that contributes to higher cytosolic $[Ca^{2+}]$. See text for details.

because this channel is overexpressed in *mdx* muscle (Gervásio et al., 2008), and we demonstrated that it operates as a SR Ca^{2+} leak channel in muscle fibers overexpressing TRPC1 (Berbey et al., 2009).

In conclusion, this paper demonstrates that the magnitude and the voltage dependence of depolarization-activated SR Ca^{2+} depletion are not modified in *mdx* muscle but that the reuptake activity of SR Ca^{2+}-ATPases is elevated. More importantly, this study also shows straightforwardly that the passive SR Ca^{2+} leak is higher in *mdx* muscle at resting membrane potential. A higher SR Ca^{2+} leak has important physiopathological consequences in dystrophin-deficient muscle that could be modeled as follows on the basis of our data (Fig. 7). The SR Ca^{2+} content is conditioned by the rate of the leak and by the rate of the reuptake that operates in the SR membrane, whereas, in the long term, cytosolic $[Ca^{2+}]$ is strictly dependent on sarcolemmal influx and efflux (Ríos, 2010). In control fibers, it can be assumed that SR leak and reuptake and sarcolemmal influx and efflux are balanced so that cytosolic $[Ca^{2+}]$ remains in the physiological resting range. In *mdx* fibers, the elevated SR leak that we measured may be no more balanced by reuptake, although this uptake was increased, probably by compensatory mechanisms. This unbalanced elevated leak may result in a chronic SR depletion that in turn overactivates sarcolemmal Ca^{2+} influx via SOCE, the activation threshold of which is, moreover, reduced (Edwards et al., 2010). It also cannot be excluded that an elevated SR leak could directly influence sarcolemmal Ca^{2+} influx independently of the SR Ca^{2+} content and SOCE. Eventually, the elevated sarcolemmal Ca^{2+} influx that transiently dominates over the efflux brings cytosolic $[Ca^{2+}]$ to a new sustained elevated set point in *mdx* fibers. Elevated sarcolemmal influx and efflux then again balance each other, maintaining chronic Ca^{2+} overload in *mdx* fibers.

We thank Vincent Jacquemond and Maelle Jospin for critical comments on the manuscript.

This work was supported by grants from the Université Lyon 1, the Centre National de la Recherche Scientifique, and the Association Française contre les Myopathies.

Richard L. Moss served as editor.

Submitted: 9 November 2011
Accepted: 9 February 2012

REFERENCES

Allard, B. 2006. Sarcolemmal ion channels in dystrophin-deficient skeletal muscle fibres. *J. Muscle Res. Cell Motil.* 27:367–373. http://dx.doi.org/10.1007/s10974-006-9083-4

Allen, D.G., O.L. Gervasio, E.W. Yeung, and N.P. Whitehead. 2010. Calcium and the damage pathways in muscular dystrophy. *Can. J. Physiol. Pharmacol.* 88:83–91. http://dx.doi.org/10.1139/Y09-058

Bellinger, A.M., S. Reiken, C. Carlson, M. Mongillo, X. Liu, L. Rothman, S. Matecki, A. Lacampagne, and A.R. Marks. 2009. Hypernitrosylated ryanodine receptor calcium release channels are leaky in dystrophic muscle. *Nat. Med.* 15:325–330. http://dx.doi.org/10.1038/nm.1916

Berbey, C., and B. Allard. 2009. Electrically silent divalent cation entries in resting and active voltage-controlled muscle fibers. *Biophys. J.* 96:2648–2657. http://dx.doi.org/10.1016/j.bpj.2009.01.008

Berbey, C., N. Weiss, C. Legrand, and B. Allard. 2009. Transient receptor potential canonical type 1 (TRPC1) operates as a sarcoplasmic reticulum calcium leak channel in skeletal muscle. *J. Biol. Chem.* 284:36387–36394. http://dx.doi.org/10.1074/jbc.M109.073221

Blake, D.J., A. Weir, S.E. Newey, and K.E. Davies. 2002. Function and genetics of dystrophin and dystrophin-related proteins in muscle. *Physiol. Rev.* 82:291–329.

Boittin, F.X., O. Petermann, C. Hirn, P. Mittaud, O.M. Dorchies, E. Roulet, and U.T. Ruegg. 2006. Ca^{2+}-independent phospholipase A2 enhances store-operated Ca^{2+} entry in dystrophic skeletal muscle fibers. *J. Cell Sci.* 119:3733–3742. http://dx.doi.org/10.1242/jcs.03184

Camello, C., R. Lomax, O.H. Petersen, and A.V. Tepikin. 2002. Calcium leak from intracellular stores–the enigma of calcium signalling. *Cell Calcium.* 32:355–361. http://dx.doi.org/10.1016/S0143416002001926

Collet, C., B. Allard, Y. Tourneur, and V. Jacquemond. 1999. Intracellular calcium signals measured with indo-1 in isolated skeletal muscle fibres from control and *mdx* mice. *J. Physiol.* 520:417–429. http://dx.doi.org/10.1111/j.1469-7793.1999.00417.x

DiFranco, M., C.E. Woods, J. Capote, and J.L. Vergara. 2008. Dystrophic skeletal muscle fibers display alterations at the level of calcium microdomains. *Proc. Natl. Acad. Sci. USA.* 105:14698–14703. http://dx.doi.org/10.1073/pnas.0802217105

Divet, A., and C. Huchet-Cadiou. 2002. Sarcoplasmic reticulum function in slow- and fast-twitch skeletal muscles from *mdx* mice. *Pflugers Arch.* 444:634–643. http://dx.doi.org/10.1007/s00424-002-0854-5

Edwards, J.N., O. Friedrich, T.R. Cully, F. von Wegner, R.M. Murphy, and B.S. Launikonis. 2010. Upregulation of store-operated Ca^{2+} entry in dystrophic mdx mouse muscle. *Am. J. Physiol. Cell Physiol.* 299:C42–C50. http://dx.doi.org/10.1152/ajpcell.00524.2009

Eltit, J.M., H. Li, C.W. Ward, T. Molinski, I.N. Pessah, P.D. Allen, and J.R. Lopez. 2011. Orthograde dihydropyridine receptor signal

regulates ryanodine receptor passive leak. *Proc. Natl. Acad. Sci. USA.* 108:7046–7051. http://dx.doi.org/10.1073/pnas.1018380108

Fong, P.Y., P.R. Turner, W.F. Denetclaw, and R.A. Steinhardt. 1990. Increased activity of calcium leak channels in myotubes of Duchenne human and *mdx* mouse origin. *Science.* 250:673–676. http://dx.doi.org/10.1126/science.2173137

Franco, A. Jr., and J.B. Lansman. 1990. Calcium entry through stretch-inactivated ion channels in *mdx* myotubes. *Nature.* 344:670–673. http://dx.doi.org/10.1038/344670a0

Gailly, P. 2002. New aspects of calcium signaling in skeletal muscle cells: implications in Duchenne muscular dystrophy. *Biochim. Biophys. Acta.* 1600:38–44.

Gervásio, O.L., N.P. Whitehead, E.W. Yeung, W.D. Phillips, and D.G. Allen. 2008. TRPC1 binds to caveolin-3 and is regulated by Src kinase - role in Duchenne muscular dystrophy. *J. Cell Sci.* 121: 2246–2255. http://dx.doi.org/10.1242/jcs.032003

Guerrero-Hernandez, A., A. Dagnino-Acosta, and A. Verkhratsky. 2010. An intelligent sarco-endoplasmic reticulum Ca^{2+} store: release and leak channels have differential access to a concealed Ca^{2+} pool. *Cell Calcium.* 48:143–149. http://dx.doi.org/10.1016/j.ceca.2010.08.001

Hollingworth, S., U. Zeiger, and S.M. Baylor. 2008. Comparison of the myoplasmic calcium transient elicited by an action potential in intact fibres of *mdx* and normal mice. *J. Physiol.* 586:5063–5075. http://dx.doi.org/10.1113/jphysiol.2008.160507

Jiménez-Moreno, R., Z.M. Wang, M.L. Messi, and O. Delbono. 2010. Sarcoplasmic reticulum Ca^{2+} depletion in adult skeletal muscle fibres measured with the biosensor D1ER. *Pflugers Arch.* 459:725–735. http://dx.doi.org/10.1007/s00424-009-0778-4

Kabbara, A.A., and D.G. Allen. 2001. The use of the indicator fluo-5N to measure sarcoplasmic reticulum calcium in single muscle fibres of the cane toad. *J. Physiol.* 534:87–97. http://dx.doi.org/10.1111/j.1469-7793.2001.00087.x

Kargacin, M.E., and G.J. Kargacin. 1996. The sarcoplasmic reticulum calcium pump is functionally altered in dystrophic muscle. *Biochim. Biophys. Acta.* 1290:4–8. http://dx.doi.org/10.1016/0304-4165(95)00180-8

Mallouk, N., V. Jacquemond, and B. Allard. 2000. Elevated subsarcolemmal Ca2+ in mdx mouse skeletal muscle fibers detected with Ca2+-activated K+ channels. *Proc. Natl. Acad. Sci. USA.* 97:4950–4955. http://dx.doi.org/10.1073/pnas.97.9.4950

Plant, D.R., and G.S. Lynch. 2003. Depolarization-induced contraction and SR function in mechanically skinned muscle fibers from dystrophic mdx mice. *Am. J. Physiol. Cell Physiol.* 285:C522–C528.

Pouvreau, S., L. Csernoch, B. Allard, J.M. Sabatier, M. De Waard, M. Ronjat, and V. Jacquemond. 2006. Transient loss of voltage control of Ca^{2+} release in the presence of maurocalcine in skeletal muscle. *Biophys. J.* 91:2206–2215. http://dx.doi.org/10.1529/biophysj.105.078089

Pouvreau, S., C. Collet, B. Allard, and V. Jacquemond. 2007. Whole-cell voltage clamp on skeletal muscle fibers with the silicone-clamp technique. *Methods Mol. Biol.* 403:185–194. http://dx.doi.org/10.1007/978-1-59745-529-9_12

Ríos, E. 2010. The cell boundary theorem: a simple law of the control of cytosolic calcium concentration. *J. Physiol. Sci.* 60:81–84. http://dx.doi.org/10.1007/s12576-009-0069-z

Ruegg, U.T., V. Nicolas-Métral, C. Challet, K. Bernard-Hélary, O.M. Dorchies, S. Wagner, and T.M. Buetler. 2002. Pharmacological control of cellular calcium handling in dystrophic skeletal muscle. *Neuromuscul. Disord.* 12:S155–S161. http://dx.doi.org/10.1016/S0960-8966(02)00095-0

Sztretye, M., J. Yi, L. Figueroa, J. Zhou, L. Royer, P. Allen, G. Brum, and E. Ríos. 2011. Measurement of RyR permeability reveals a role of calsequestrin in termination of SR $Ca^{(2+)}$ release in skeletal muscle. *J. Gen. Physiol.* 138:231–247. http://dx.doi.org/10.1085/jgp.201010592

Takagi, A., S. Kojima, M. Ida, and M. Araki. 1992. Increased leakage of calcium ion from the sarcoplasmic reticulum of the *mdx* mouse. *J. Neurol. Sci.* 110:160–164. http://dx.doi.org/10.1016/0022-510X(92)90023-E

Turner, P.R., T. Westwood, C.M. Regen, and R.A. Steinhardt. 1988. Increased protein degradation results from elevated free calcium levels found in muscle from *mdx* mice. *Nature.* 335:735–738. http://dx.doi.org/10.1038/335735a0

Tutdibi, O., H. Brinkmeier, R. Rüdel, and K.J. Föhr. 1999. Increased calcium entry into dystrophin-deficient muscle fibres of MDX and ADR-MDX mice is reduced by ion channel blockers. *J. Physiol.* 515:859–868. http://dx.doi.org/10.1111/j.1469-7793.1999.859ab.x

Vandebrouck, C., D. Martin, M. Colson-Van Schoor, H. Debaix, and P. Gailly. 2002. Involvement of TRPC in the abnormal calcium influx observed in dystrophic (mdx) mouse skeletal muscle fibers. *J. Cell Biol.* 158:1089–1096. http://dx.doi.org/10.1083/jcb.200203091

Wang, X., N. Weisleder, C. Collet, J. Zhou, Y. Chu, Y. Hirata, X. Zhao, Z. Pan, M. Brotto, H. Cheng, and J. Ma. 2005. Uncontrolled calcium sparks act as a dystrophic signal for mammalian skeletal muscle. *Nat. Cell Biol.* 7:525–530. http://dx.doi.org/10.1038/ncb1254

Woods, C.E., D. Novo, M. DiFranco, and J.L. Vergara. 2004. The action potential-evoked sarcoplasmic reticulum calcium release is impaired in *mdx* mouse muscle fibres. *J. Physiol.* 557:59–75. http://dx.doi.org/10.1113/jphysiol.2004.061291

Ziman, A.P., C.W. Ward, G.G. Rodney, W.J. Lederer, and R.J. Bloch. 2010. Quantitative measurement of $Ca^{2}(+)$ in the sarcoplasmic reticulum lumen of mammalian skeletal muscle. *Biophys. J.* 99:2705–2714. http://dx.doi.org/10.1016/j.bpj.2010.08.032